ENVIRONMENTAL ENGINEERING SCIENCE
Volume 00, Number 00, 2018

DOI: 10.1089/ees.2017.0539

ORIGINAL ARTICLE

Effects of Ultrasound on Removal of Ranitidine Hydrochloride from Water by Activated Carbon Based on *Lagenaria siceraria*

Miloš M. Kostić,[1,*] Andrew P. Hurt,[2] Dragan D. Milenković,[3] Nena D. Velinov,[1] Milica M. Petrović,[1] Danijela V. Bojić,[1] Dragana Z. Marković-Nikolić,[4] and Aleksandar Lj. Bojić[1]

[1]*Department of Chemistry, Faculty of Science and Mathematics, University of Niš, Niš, Serbia.*
[2]*Faculty of Engineering and Science, University of Greenwich, Chatham Maritime, Kent, United Kingdom.*
[3]*Department of Chemical Technology, High Chemical Technological School, University of Niš, Kruševac, Serbia.*
[4]*High Technology Arts Vocational School, University of Niš, Leskovac, Serbia.*

Received: December 21, 2017 *Accepted in revised form: May 7, 2018*

Abstract

Sorption removal of ranitidine hydrochloride (RH) from aqueous solution, using activated carbon obtained from *Lagenaria siceraria* activated carbon (LSAC), in the presence and absence of ultrasound, was investigated in batch mode. Characterization of material by Brunauer–Emmett–Teller analysis shows high surface area of 665 m^2/g. The value of pH_{PZC} is found to be 7.2. The Fourier transform infrared spectroscopy spectrum is typical for carbon materials. Scanning electron microscopy and energy-dispersive X-ray spectroscopy (EDS) analyses show porous, sponge-like, and amorphous structure, with high carbon content, and very small amount of oxygen. In addition, Boehm's analysis indicates relatively small amount of oxygen functional groups. Time for sorption equilibrium was about six times shorter in presence of ultrasound. The Langmuir isotherm and pseudo-second order kinetic model the best describe the RH removal process, indicating monolayer sorption. Sorption capacity of LSAC increases by influence of ultrasound, and maximal sorption capacities are 328.71, 389.84, and 425.43 mg/g for power of 0, 25, and 50 W, respectively. When temperature increased from 10°C to 30°C, sorption capacity decreased. Thermodynamic analysis showed that sorption was exothermic and spontaneous, implying the physisorption mechanism of RH removal by LSAC.

Keywords: activated carbon; *Lagenaria siceraria*; ranitidine hydrochloride; sorption; ultrasound; pollution

Introduction

Drugs such as antibiotics, hormones, anesthetics, antilipemics, anti-inflammatories, and others have been detected in wastewater and surface and ground water (Dezotti and Bila, 2003; Tejeda *et al.*, 2017). One of the most commonly used drugs of today is ranitidine, because of a wide population suffering from gastric diseases.

Ranitidine hydrochloride (RH) is a histamine H2 receptor antagonist, used to treat and prevent ulcers in the stomach and intestines and the Zollinger–Ellison syndrome (the production of too much acid). RH is excreted from the organism by urine and feces and is discharged into communal water using the sewage system. Due to this process, it later emerges in surface waters, mainly rivers and lakes. The presence of RH can affect the aquatic organisms that have the same enzymatic receptors and thereby produce the same pharmacodynamic effects. The presence of very low quantities of RH or its derivatives is therefore highly undesirable for the aquatic system (Vediappan and Lee, 2011).

RH is classified as a drug with hazardous effects on the environment, so it is essential to remove it from wastewater before discharging it into the environment due to its occurrence in a variety of aquatic environments. RH is only partially biodegradable, and sunlight can also partially change its structure, giving persistent and toxic photoproducts (Bergheim *et al.*, 2012; Sivarajasekar *et al.*, 2017a). Conventional techniques such as physical and chemical treatments (bioremediation, coagulation, volatilization, sedimentation, filtration etc.) are some of the methods used to treat wastewaters containing drugs. However, high costs and the impossibility of complete removal have forced researchers to focus their investigations on alternative techniques. Sorption is observed to be one of the most promising techniques due to its convenience and low cost (Sivarajasekar *et al.*, 2017a).

Up to now, sorption of various drugs onto activated carbon (Baccar *et al.*, 2012), zeolites (Martucci *et al.*, 2012), chitosan (Kyzas *et al.*, 2013), clays (Figueroa *et al.*, 2004), and silica (Bui and Choi, 2010) has been explored.

Ultrasound through its mechanical waves has been used as a means for enhancing the sorption process. When ultrasound is irradiated through a liquid, it induces very small gas

**Corresponding author:* Department of Chemistry, Faculty of Sciences and Mathematics, University of Niš, Višegradska 33, Niš 18 000, Serbia. *Phone:* +381 63 48 44 75; *Fax:* +381 16 260 437; *E-mail:* mk484475@gmail.com

bubbles to oscillate, which under appropriate conditions leads to the growth and sudden collapse of microbubbles in the rarefaction cycle of the ultrasonic wave, when strong negative pressure is applied to the liquid. This is referred to as acoustic cavitation (symmetric and asymmetric) and leads to high localized temperatures and pressures inside the cavity (Adewuyi, 2001). Asymmetric collapse can lead to particle size reduction or ''surface erosion,'' which can contribute to the creation of active sites on solid particle surfaces (Mason *et al.*, 1996).

Ultrasonic waves strongly enhance mass transfer between two phases through reducing the thickness of liquid films at the solid phase, after which the diffusion is enhanced (Entezari and Keshavarzi, 2001). Ultrasonic waves have a greater efficiency for interface mixing than conventional agitation.

This study reports novel experimental and theoretical studies of the effects of ultrasound on removal of RH from aqueous solution by sorption using thermochemically synthesized activated carbon based on *Lagenaria siceraria* (LSAC), as an alternative low-cost sorbent. Kinetics, equilibrium, and thermodynamic modeling of experimental results were carried out. Besides the effects of ultrasound (acoustic power), various operational parameters such as agitation speed, sorbent dosage, contact time, and temperature were also studied and optimized under the batch conditions. Application of ultrasound shows double effects: decrease of equilibrium time and increase of sorption capacity. Unlike the most previously used sorbents, the advantage of this sorbent is the efficient removal of RH in a very wide pH range.

Materials and Methods

Reagents

HNO_3, H_2SO_4, and NaOH were purchased from Merck (Germany). The active substance RH was obtained from Sigma-Aldrich (Germany) with >99% purity. Stock solution of RH ($C_{13}H_{22}N_4O_3S \cdot HCl$; Mr = 350.87 g/mol) of 1,000 mg/dm^3 was prepared by dissolving appropriate amounts of substance in 1,000 cm^3 deionized water. This stock solution was used for preparing a series of drug concentrations ranging from 20 to 600 mg/dm^3.

Thermochemical synthesis of activated carbon

Activated carbon used in this study was prepared of *Lagenaria siceraria* shell. It is a hardy climbing plant which is mainly grown on alluvial sandy soil, and it belongs to the family *Cucurbitaceae*. Fresh picked fruits are dried for about 3 months at the outside temperature in shade. After drying, fruits were manually emptied from seeds and the spongy white pith characterized by its bitter taste. Outer shell was crushed into 2–3 cm pieces and cleansed of the rest of internal content. Small pieces of broken shell were washed several times with deionized water to remove dust and soil and then dried at 60°C.

The dried pieces of shell were grounded using a laboratory mill (Waring, Germany) and sieved (Endecotts, England) to the particle size in the range from 0.80 to 1.25 mm. The biomass was further immersed in 10% H_2SO_4 and stirred occasionally within 48 h. The resulting precursor was washed several times with deionized water until neutral pH and dried.

The further synthesis of activated carbon happens in two phases. In the first phase, the obtained precursor was carbonized in a tubular furnace under the protective atmosphere of nitrogen by being heated from room temperature to 400°C for 1 h. After that followed the second phase (activation) when the precursor was activated by introducing overheated steam into the furnace at flow of 110 cm^3/min with gradually increasing the temperature from 400 to 700°C. In next step the temperature was maintained constant at 700°C for 1 h. After activation, the furnace was spontaneously cooled down in inert atmosphere. Obtained *Lagenaria siceraria* activated carbon (LSAC) was washed with deionized water and dried for 2 h and stored in a closed bottle.

Characterization of sorbent

Specific surface area was measured by a nitrogen adsorption using the Surface Area Analyzer Micromeritics Gemini 5 (USA) and determined by The Brunauer–Emmett–Teller (BET) mathematical isotherm model. The surface oxygen groups on a carbon with acidic (carboxyl, lactone, phenol), as well as basic, properties can be determined by the Boehm method. These groups differ in their acidity and can be distinguished by neutralization with different solutions: HCl and $NaHCO_3$, Na_2CO_3 and NaOH. The method was in detail described in the previous study (Bojić *et al.*, 2015).

Infrared analysis of LSAC was obtained using a Fourier transform infrared spectrometer (Bomem Hartmann & Braun MB -100 spectrometer, Canada). A Hitachi SU8030 cold field mission gun scanning electron microscopy (SEM) was used for imaging the samples with Thermo-Noran NSS system 7 ultradry X-ray detectors for semiquantitative energy-dispersive X-ray spectroscopy (EDS) analysis. The crystalline structure of the samples was investigated using X-ray diffraction (XRD). The XRD patterns were recorded with a Bruker D8 Advance X-ray Diffractometer (Bruker, Germany).

Batch mode sorption studies

Batch sorption experiments were conducted in the experimental setup shown in Fig. 1. The setup consisted of an ultrasonic bath (Sonic, Serbia; total nominal power 50 W) operating at 40 kHz. All experiments were carried out at the temperature ranging from 10°C to 30°C (±0.2°C) in the ultrasonic bath thermostated by recirculating water from refrigerated/heating circulator Julabo F12-ED (Germany). The native pH values of solutions were from 5 to 6.2 and were not additionally adjusted during the treatment, because the effect of pH on RH sorption onto *Lagenaria vulgaris* carbon is negligible (Bojić *et al.*, 2015).

Effect of LSAC dose. Effect of the sorbent dose on the removal efficiency (RE) of RH, at initial concentration of 150 mg/dm^3, was investigated with LSAC concentrations of 0.25, 0.5, 0.75, 1.0, and 2.0 g/dm^3 at acoustic power of 0, 25, and 50 W. The experiments were performed at the stirring speed of 200 rpm at the temperature of 20°C to the equilibrium uptake (3 h) where the concentration change of RH was determined by the spectrophotometric method.

Effects of hydrodynamic conditions: ultrasound and steering speed. Effects of hydrodynamic conditions were investigated by the use of ultrasound and stirring, combined and

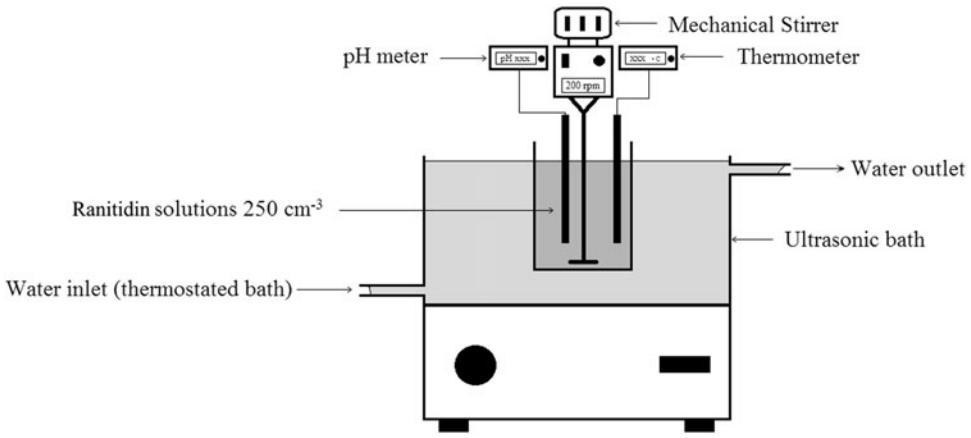

FIG. 1. Scheme of experimental setup used for the sorption of RH by LSAC. LSAC, *Lagenaria siceraria* activated carbon; RH, ranitidine hydrochloride.

independently, with all other parameters constant (the temperature was 20°C, the RH concentration was 150 mg/dm^3, and the sorbent dose 1.0 g/dm^3). The effect of stirring speed on RH sorption was investigated in the range from 50 to 400 rpm and by the combination of stirring and ultrasound power of 25 and 50 W.

Kinetics and isotherm studies. All batch sorption experiments were performed in 250 cm^3 of working volume of sample with initial RH concentrations of 20, 150, 300, 400, and 600 mg/dm^3 and 0.25 g of activated carbon LSAC (sorbent dosage 1.0 g/dm^3), with the stirring speed of 200 rpm. Ultrasonic waves were used for sonication experiments at three different ultrasonic powers: 0, 25, and 50 W, as measured by calorimetry (Kimura *et al.*, 1996).

The experiments were conducted at 20°C. Samples were taken from the flask at a specified time interval (0, 0.5, 1, 5, 10, 20, 40, 60, 90, 120, and 180 min), centrifuged, filtered using 0.45 μm regenerated cellulose membrane filter (Agilent Technologies, Germany), and analyzed using the direct UV-vis technique by spectrophotometer Shimadzu UV-vis 1650 PC (Shimadzu, Japan) at 313 nm, with the detection limit of 1.0 mg/dm^3. Low RH concentrations were determined by the spectrophotometric method based on the addition of ceric ammonium sulfate and dye crystal violet with measuring absorbance at 582 nm (detection limit 0.1 mg/dm^3).

The *RE* of RH by activated carbon was calculated using Equation (1):

$$RE\,\% = \frac{c_0 - c_t}{c_0} \times 100 \tag{1}$$

The amount of drug sorbed q_t (mg/g) was determined using the following equation:

$$q_t = \frac{(c_0 - c_t)}{m} \times V \tag{2},$$

where c_0 and c_t are the initial and final concentrations of the RH in the solution (mg/dm^3), V is the solution volume (dm^3), and m is the mass of the LSAC (g).

Kinetic investigations were conducted using pseudo-first order (Lagergren, 1898), pseudo-second order (Ho and McKay, 1998), Chrastil (1990), and intraparticle diffusion models (Zhou *et al.*, 2017).

The batch equilibrium data were fitted to isotherms such as Langmuir (Sivarajasekar *et al.*, 2017b), Freundlich (Sivarajasekar *et al.*, 2017b), Temkin and Pyzhev (1940), Sips (1948), and Brouers-Sotolongo (Brouers *et al.*, 2005), which were applied in different ultrasound powers.

To ensure the accuracy, reliability, and reproducibility of the collected data, all experiments were carried out in triplicate, and mean values are recorded. OriginPro 2016 (OriginLab Corporation) software was used to fit the kinetics and equilibrium models using nonlinear regression.

Effect of temperature and thermodynamics. Effect of temperature on the RH sorption experiments was investigated at three different temperatures (283, 293, and 303 K). The initial concentration was 600 mg/dm^3, and acoustic power was 0, 25, and 50 W.

To determine spontaneity and heat change for the sorption reactions, thermodynamic parameters were calculated. The change of free energy ΔG° was calculated using the following equation:

$$\Delta G^\circ = -\mathrm{R}T \ln K_D \tag{3}$$

$$\Delta G^\circ = \Delta H^\circ - T\Delta S^\circ \tag{4}$$

The enthalpy (ΔH°) and entropy (ΔS°) parameters were estimated from the following equation:

$$\ln K_\mathrm{D} = \frac{\Delta S^\circ}{\mathrm{R}} - \frac{\Delta H^\circ}{\mathrm{R}T} \tag{5},$$

where R is the universal gas constant (8.314 J/[mol K]), T is the temperature (K), and K_D is the coefficient of distribution.

$$K_\mathrm{D} = \frac{c_a}{c_e} \tag{6},$$

where c_a and c_e are the RH concentration (mg/dm^3) on the sorbent at equilibrium condition and in the solution, respectively.

According to Equation (5), enthalpy change and entropy change were calculated, respectively, from the slop and intercept of the plots of $1/T$ versus $\ln K_\mathrm{D}$ (Mondal *et al.*, 2017; Sivarajasekar *et al.*, 2017c).

Results and Discussion

Characterizations of LSAC

The surface area of LSAC was measured by BET nitrogen sorption technique. N_2 adsorption/desorption isotherm for LSAC is a classical IV-type of isotherm with N_2 hysteresis loops, revealing the presence of mesoporous structures according to the IUPAC classification. LSAC has relatively high BET surface area of 665 m^2/g, which is probably due to well developed porosity, predominantly represented by micropores. The BET results also showed that the micropore volume of LSAC was 0.302 cm^3/g, and the mesopore volume was 0.08 cm^3/g. The mesopore area measured by the t-plot method was 73 m^2/g. By the Barret-Joyner-Halenda method, the dominant size of the LSAC pores is around 2.2 nm. The big surface area and microporous structure of LSAC provide numerous active sites for sorption of organic pollutants on its surface and enable the effective diffusion.

In order to elucidate the acid-base character of the LSAC surface, Boehm's titrations and pH_{PZC} analysis of activated carbon were done. Boehm's analysis of LSAC showed that the process of thermal carbonization and activation significantly influenced the change in the proportion of different oxygen functional groups and their molar relationship. These processes involve introduction of acidic functional groups in the structure of the final material. The very acidic groups such as carboxylic make almost 50% of all oxygen groups in the LSAC, based on Boehm's analysis. The molar ratio of strongly acidic groups has increased most probably due to activation by steam, which has oxidative effects. In contrast, the surface concentration of very weak acidic groups (phenolic groups) is almost unchanged compared to precursor (Bojić *et al.*, 2015).

According to the results of Boehm's analysis, activated carbon LSAC has a relatively small amount of oxygen functional groups, which increases the hydrophobicity of surface and affinity for nonpolar and weakly polar substances. The value of pH_{PZC} (determined by drift method (Bojić *et al.*, 2015)) for LSAC is found to be 7.2.

Discussion of Fourier transform infrared spectroscopy (FTIR) analysis of precursor (*Lagenaria siceraria* shell) was previously reported (Bojić *et al.*, 2015), where it can be noticed well defined characteristic bands in FTIR spectrum. FTIR spectra of LSAC before and after sorption of RH are shown in Fig. 2. The broadband at around 3,400 cm^{-1} is typically attributed to hydroxyl groups. The absorption peak around 1,600 cm^{-1} in LSAC spectrum before sorption RH indicates the C = C stretching vibrations from aromatic rings of lignin. During carbonization at 700°C, the most peaks get lower intensity, some disappear, reducing of resolution, and increasing the noise happens in wide range, in comparison with FTIR spectra for noncarbonized *Lagenaria siceraria* shell (Bojić *et al.*, 2015).

FTIR spectrum of LSAC after sorption of RH shows that there is no significant shift of peaks, which indicates a physical mechanism of sorption.

Morphology and structure of the LSAC before and after sorption RH were observed by SEM (Fig. 3a, b). The SEM micrographs of samples before sorption of RH show macroporous, sponge-like, and amorphous structure. This structure results from the generation of large amounts of gas from organic and inorganic volatile compounds which arise during carbonization process, giving a dense microstructure. The larger particle, which can be seen in Fig. 3a, is only partially derived from original structure of the noncarbonized *Lagenaria siceraria* shell, while other smaller particles of irregular shape appeared by disintegration of typical structural elements of shell. The external surface is full of cavities with pores of different sizes and shapes that are visible at magnification of 2,000 times, which enables the easy penetration and sorption of RH on LSAC by the diffusion. Significant morphological changes were not observed after sorption of RH on LSAC. The amorphous morphology of LSAC was confirmed by the XRD analysis whose results showed complete absence of diffraction peaks for the crystalline phases. XRD pattern was not shown.

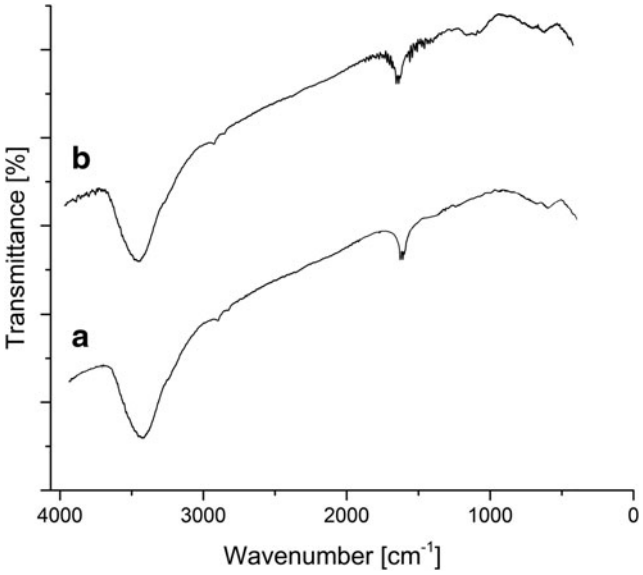

FIG. 2. Fourier transform infrared spectra of (a) before sorption of RH on LSAC and (b) after sorption of RH on LSAC.

EDS spectra of LSAC are shown in Fig. 3c. The EDS results of surface of LSAC show high carbon content, which is typical for thermally carbonated materials. At high temperature treatment, condensation of aromatic rings results in the release of low molecular weight volatile components of biomass. In this way, most of the oxygen and hydrogen are lost, which increase the carbon content. In LSAC, there is a significantly lower proportion of oxygen than other activated carbon, in which the content of this element is higher (Kaouah *et al.*, 2013). This is consistent with the results of the testing of surface functional groups such as LSAC Boehm's method, where a relatively small proportion of carboxyl, lactone, and phenolic groups is also observed, compared to similar materials.

Effects of hydrodynamic conditions: Ultrasound and steering speed

The effects of ultrasound and stirring speed on RH sorption were studied. From the Fig. 4, it is observed that the increase in agitation speed from 50 to 200 rpm resulted in an increase in RH sorption from 54.56% to 89.92%, without the presence of ultrasound. Therefore, RE increased by about 35%. The stirring speed of 200 rpm ensures efficient dispersion of

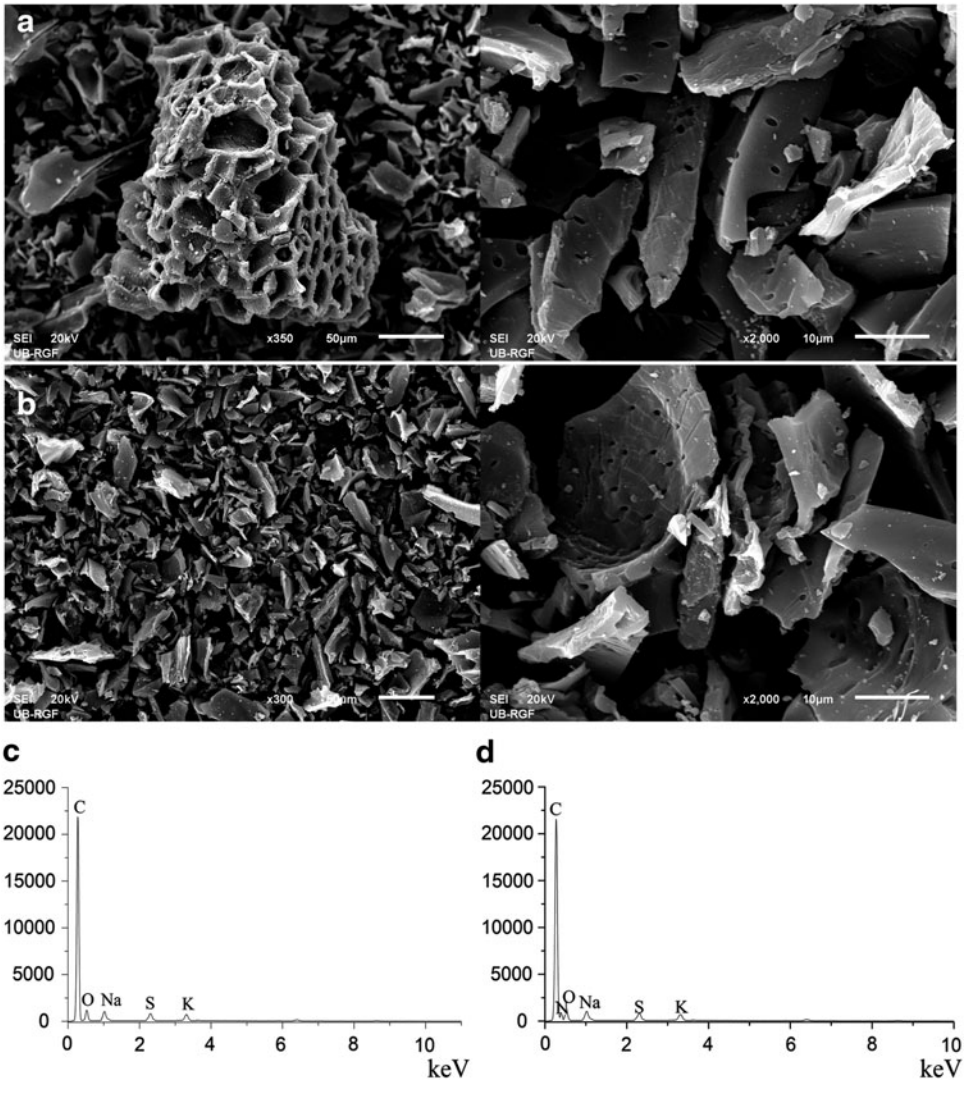

FIG. 3. **(a)** SEM micrographs of the LSAC before sorption of RH, **(b)** SEM micrographs of the LSAC after sorption of RH, **(c)** EDS spectra before sorption of RH, and **(d)** EDS spectra after sorption of RH. EDS, energy-dispersive X-ray spectroscopy; SEM, scanning electron micrographs.

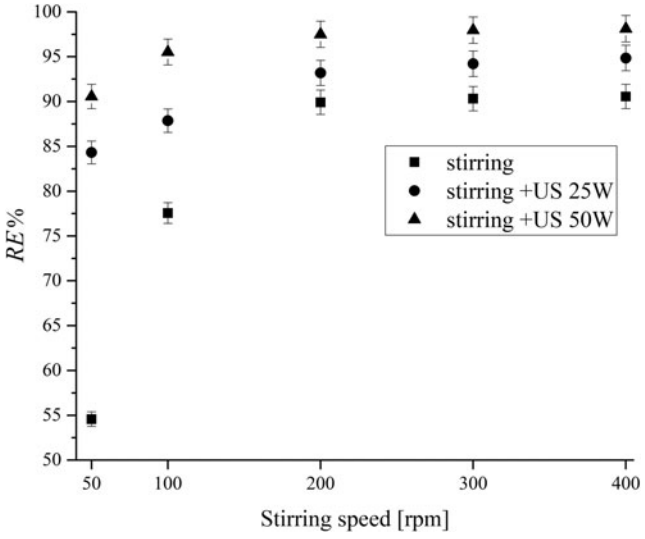

FIG. 4. Effect of ultrasound and stirring speed on the sorption of RH by LSAC.

LSAC in the liquid medium and reduces the film boundary layer surrounding the sorbent particles, thus increasing the external film mass transfer coefficient and the rate of drug sorption (Guechi and Hamdaoui, 2016). This speed was used for the rest of the study.

The RE of RH occurring through the combination of ultrasound and mechanical stirring was significantly higher than one occurring through stirring alone. The RE increased from 84.32% to 93.20% for the combined method, that is, ultrasound power of 25 W and stirring speed of 200 rpm and from 90.56% to 97.49% for the ultrasound power of 50 W and stirring speed of 200 rpm.

These effects were related to hydrodynamic phenomena occurring due to cavitation and stirring, which gave the maximal possible contact between solid and liquid phases, in applied conditions. With the increase of ultrasound power, the cavitation was more intense, while the number of cavitation events and the intensities of the high-speed microjets and of the high pressure shock waves produced by acoustic cavitation were also increased. It is obvious that the effect of stirring speed on RE is lesser when ultrasound is applied. The use of ultrasound with the power of 50 W enables one to decrease the stirring speed to 50 rpm.

Effects of contact time

Effect of contact time on the RE of RH by LSAC at various ultrasound powers was studied in intervals between 0 and 180 min (Fig. 5). The other parameters such as initial concentration, agitation speed, sorbent dosage, and temperature were kept constant at 150 mg/dm^3, 200 rpm, 1.0 g/dm^3, and 20°C, respectively. The data obtained in this step were used further for kinetic studies.

Results show that the RE increased with increasing contact time and ultrasound power. In the first 20 min the largest amount of RH present in water solution was removed, in the presence of ultrasound with the power of 25 and 50 W (Fig. 5). Without using the ultrasound, sorption of RH was much slower, and the first stage was finished after about 40 min. The second stage of RH sorption with LSAC had a lower rate in all cases, and the equilibrium time was reached for about 60 min of sorption.

The short time needed for reaching equilibrium indicates a high affinity of LSAC for the pollutant especially in the presence of ultrasound. The time required for reaching the equilibrium without the ultrasound was 60 min, for US power of 25 W was 20 min, and for 50 W it was 10 min. It is obvious that the sorption time for equilibrium was about six times shorter under the influence of ultrasound, which is a very important parameter for water purification (Krika *et al.* 2016).

It is assumed that the sorption was more effective in the presence of ultrasound because of the reduction of the film boundary layer and increase of diffusion (primary effect). The secondary effect was cavitation, that is, the formation, growth, and implosive collapse of bubbles in the liquid medium (Hamdaoui *et al.*, 2003). When the bubble is implosive, collapsing near the solid surface in the liquid medium, the collapse occurs asymmetrically while symmetric cavitation is hindered. The asymmetric collapse of bubbles produces high-speed microjets.

Collapse of bubbles generates shockwaves, which cause extremely turbulent flow at the liquid–solid interface, increasing the rate of mass transfer near the solid surface. The cavitation process increases the diffusion process by the microjet and streaming produced in the collapse of the cavity, therefore leading to an improvement of the sorption by an enhancement of mass transfer across the boundary layer, as well as into the pores. This was attributed to the cavitation effects, which increase the capability of the porous particle structure for RH sorption and to the appearance of new sites of sorption by disruption of sorbent particles or new sites into the pores. The new sites, that were unavailable at silent sorption (due to insufficiently efficient diffusion), become available by increasing the efficiency of the diffusion process using ultrasound.

A blank assay without LSAC (effects of ultrasound on RH) was run. The experiment targeting the potential degradation of RH using ultrasound was conducted at the RH concentration of 600 mg/dm^3, acoustic power of 50 W, stirring speed of 200 rpm, and temperature of 20°C, in the period of 6 h. Results showed that there are no significant changes in concentration of RH in the solution without sorbent (result not shown).

Effect of LSAC dosage

The effect of sorbent dose of LSAC on the RE of RH at equilibrium is shown in Fig. 6. As expected, the percentage of RH removal increased with increasing the LSAC dosage at the constant initial concentration of RH, for all applied acoustic powers and stirring speeds. Increase of sorption with the increase of the LSAC dose was attributed to the availability of larger surface area and more sorption sites. It was observed that the sorption percentage increased from 80.46% to 89.92% with the LSAC dosage from 0.2 to 1.0 g for the acoustic power of 0, from 86.26% to 93.20% for dosage 0.2–0.75 with the acoustic power of 25 W, and from 93.26% to 97.19% (dosage 0.2–0.75) for 50 W. For the sorbent dosage of 1.0 g/dm^3 the RE increased for about 10% in the presence of ultrasound acoustic power of 50 W compared to results in the absence of ultrasound.

The increase of RH RE with the sorbent dosage can be attributed to the increase of activated carbon surface and thus the number of sorption sites (Omri *et al.*, 2016). With further increase of LSAC concentration, the RE becomes unchanged,

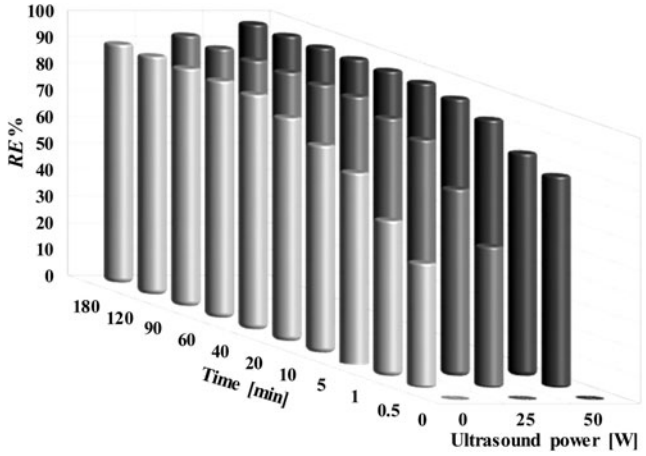

FIG. 5. Effect of contact time on sorption of RH onto LSAC using different ultrasound power.

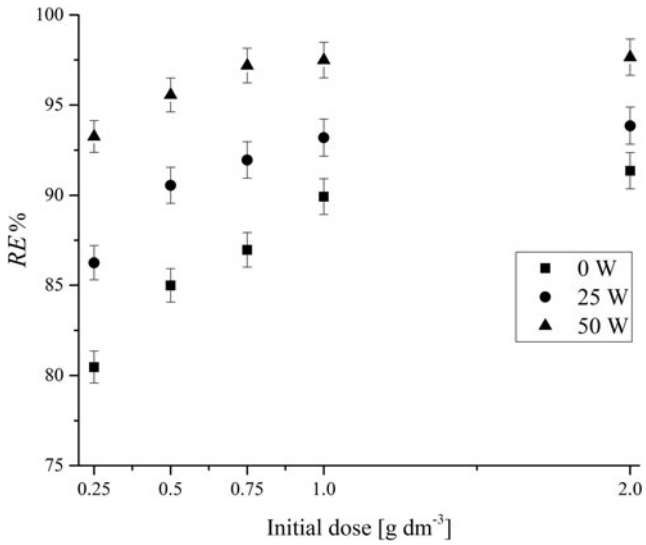

FIG. 6. Influence of LSAC dose on removal efficiency of RH.

Table 1. Values of Kinetic Parameters for Applied Kinetic Models

Acoustic power [W]		*20 [mg/dm^3]*	*150 [mg/dm^3]*	*300 [mg/dm^3]*	*400 [mg/dm^3]*	*600 [mg/dm^3]*
0	$q_{e\ (exp)}$ [mg/g]	19.54	134.88	234.07	274.91	310.72
25	$q_{e\ (exp)}$ [mg/g]	19.64	139.79	248.79	308.07	369.12
50	$q_{e\ (exp)}$ [mg/g]	19.90	146.24	277.17	347.64	423.87
Pseudo-first order $q_t = q_e(1 - e^{-k_1 t})$						
0	k_1[min^{-1}]	4.240	1.358	2.101	2.612	2.576
	q_e [mg/g]	19.26	127.70	218.94	261.48	296.69
	r^2	0.996	0.949	0.948	0.973	0.966
	k_1[min^{-1}]	5.664	1.631	2.298	2.889	1.837
25	q_e [mg/g]	19.58	136.46	231.29	294.41	347.37
	r^2	1	0.990	0.955	0.972	0.967
	k_1[min^{-1}]	5.533	3.193	1.894	1.603	1.796
50	q_e [mg/g]	19.87	143.92	265.07	332.75	397.28
	r^2	1	0.986	0.980	0.980	0.974
Pseudo-second order $q_t = \frac{k_2 q_e^2 t}{1 + k_2 q_e t}$						
	k_2 [g/mg·min]	0.748	0.015	0.017	0.021	0.018
0	q_e [mg/g]	19.41	131.57	223.32	265.48	301.51
	r^2	1	0.992	0.985	0.988	0.986
	k_2 [g/mg·min]	1.785	0.020	0.019	0.022	0.009
25	q_e [mg/g]	19.64	139.28	235.39	298.74	354.68
	r^2	1	0.998	0.991	0.988	0.987
	k_2 [g/mg·min]	1.697	0.056	0.013	0.008	0.008
50	q_e [mg/g]	19.93	145.67	269.95	340.33	405.54
	r^2	1	0.997	0.996	0.993	0.985
Chrastil model $q_t = q_e(1 - e^{-k_c A_0 t})^n$						
0	q_e [mg/g]	19.42	134.52	234.15	273.90	308.47
	n	0.053	0.172	0.085	0.064	0.075
	k_c [dm^3/g·min]	0.233	0.064	0.022	0.026	0.044
	r^2	1	0.997	0.999	0.998	0.998
25	q_e [mg/g]	19.59	138.36	246.02	273.90	361.52
	n	0.293	0.235	0.073	0.058	0.122
	k_c [dm^3/g·min]	3.358	0.268	0.020	0.027	0.064
	r^2	1	0.993	0.998	1	0.993
50	q_e [mg/g]	19.88	146.30	271.06	341.13	413.29
	n	0.482	0.074	0.146	0.185	0.120
	k_c [dm^3/g·min]	4.146	0.138	0.137	0.145	0.059
	r^2	1	1	0.995	0.987	0.980
Intraparticle diffusion model $q_t = K_{id} t^{\frac{1}{2}} + C$						
0	K_{id1} [mg/g·min$^{0.5}$]	18.907	90.078	181.530	234.394	262.416
	C_1	0.864	1.519	6.271	8.002	9.846
	r^2	0.864	0.980	0.920	0.922	0.906
	K_{id2} [mg/g·min$^{0.5}$]	0.031	7.945	9.576	7.304	15.643
	C_2	17.992	91.235	172.255	225.286	233.179
	r^2	0.941	0.981	0.939	0.992	0.817
25	K_{id1} [mg/g·min$^{0.5}$]	20.628	107.000	194.154	267.166	281.496
	C_1	0.874	0.921	8.392	10.987	5.526
	r^2	0.882	0.995	0.877	0.888	0.973
	K_{id2} [mg/g·min$^{0.5}$]	0.085	4.986	6.401	8.671	18.837
	C_2	19.247	116.233	198.588	254.049	266.360
	r^2	0.987	0.983	0.985	0.812	0.997
50	K_{id1} [mg/g·min$^{0.5}$]	20.085	133.887	215.415	260.282	328.118
	C_1	0.255	5.665	5.285	1.464	1.878
	r^2	0.989	0.882	0.959	0.998	0.998
	K_{id2} [mg/g·min$^{0.5}$]	0.053	3.282	6.044	12.195	10.615
	C_2	19.671	131.861	235.443	276.441	338.615
	r^2	0.368	0.803	0.979	0.698	0.928

perhaps due to the overlapping or aggregation of sorption sites (Fig. 6). Higher powers of ultrasound lead to reducing the amount of the sorbent, and the optimal selected dosage is around 1.0 g/dm^3, which was used in all further experiments. Similar observations have been reported earlier (Entezari and Bastami, 2006; Mondal *et al.*, 2015). Using the ultrasound with the power of 50 W gives us the opportunity to decrease the amount of sorbent and stirring speed, that is, the optimal sorbent dose is 0.75 g/dm^3, stirring speed is 50 rpm, and time to reach equilibrium decreases to less than 10 min.

Kinetic study

Values of parameters of the kinetic models at five initial concentrations of RH and three ultrasound powers are presented in Table 1. As can be seen from Table 1, pseudo-second order and Chrastil kinetic models provide the best fitted models and also have high determination coefficient (r^2) values and the q_e value very close to the experimental q_e.

The kinetic model of pseudo-first order has a good determination coefficient (r^2) compared to other models. The theoretic values of q_e are lower than the corresponding experimental q_e, implying that the sorption process does not fully follow the pseudo-first order sorption rate expansion. Results also show that the value of the determination coefficients increases with increasing ultrasound power. Therefore, the pseudo-second order model better represented the sorption kinetics and thus supports the assumption behind the model. Comparison of the values of RH amount sorbed at equilibrium (q_e) for all the tested powers of ultrasound shows that in the presence of ultrasonic irradiation q_e increases with ultrasound power, as well as with high powers more cavitation events occur and more molecules are sorbed.

The intraparticle diffusion plots for the effects of ultrasound power on the sorption of RH onto LSAC are shown in Table 1. According to the presented results, regression of q_t versus $t^{1/2}$ for the sorption shows the multilinearity in three stages for all concentrations and all powers of ultrasound. The first linear dependency can be attributed to RH transfer from the bulk solution onto the external surface of LSAC due to the diffusion in the boundary layer (film diffusion). The second linear dependency is connected with the diffusion of RH within the pores of LSAC where intraparticle diffusion was rate limiting in the sorption step (Taleb *et al.* 2016). The latest linear dependency was attributed to the final equilibrium stage, where the diffusion slows down because of the concentration gradient that decreases with time.

The slope of the linear portion indicated the rate of the sorption, that is, as the value of k_{id} (rate constant for intraparticle diffusion) is lower, the sorption is slower. The first stage k_{id1} is the fastest, and the second stage k_{id2} (the diffusion of molecules within the pores of the sorbent) is slower and corresponding to diffusion into meso- and micropores. The last stage k_{id3} is the one with the lowest slope and indicates that the equilibrium has been reached. This implies that the intraparticle diffusion was the rate-limiting step for the sorption RH on LSAC. The intraparticle diffusion model showed that the process was controlled by the diffusion of the sorbate in the pores of the LSAC and that was the slowest step.

It was found that the rate constant (K_{id1} and K_{id2}) increased with increasing initial concentration and ultrasound power. Increase of initial concentration raises the driving force of

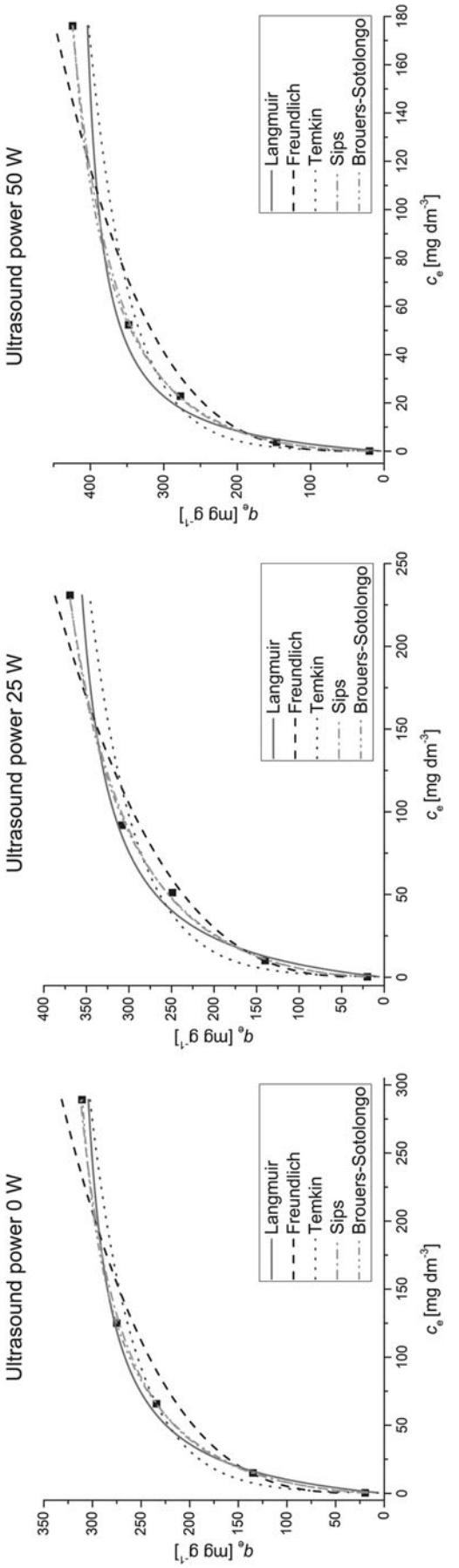

FIG. 7. Sorption isotherms of RH on LSAC.

TABLE 2. PARAMETERS OF APPLIED ISOTHERM MODELS FOR RANITIDINE HYDROCHLORIDE SORPTION ON LSAC AT 20°C

Isotherm model	*Parameter*	*Ultrasound power [W]*		
		0	*25*	*50*
Langmuir $q_e = \frac{q_m K_L c_e}{1 + K_L c_e}$	$q_{e\ (exp)}$ [mg/g]	310.72	369.12	423.87
	r^2	0.992	0.989	0.994
	K_L [dm^3/mg]	0.043	0.044	0.105
	q_{max} [mg/g]	328.71	389.84	425.43
Freundlich $q_e = K_F c_e^{\frac{1}{n}}$	r^2	0.952	0.971	0.958
	K_F [dm^3/g]	61.120	66.586	108.059
	n [g dm^{-3}]	3.351	3.091	3.639
Temkin $q_e = \frac{RT}{b_T} \ln(K_T c_t)$	r^2	0.967	0.951	0.955
	K_t [dm^3/mg]	2.475	2.705	8.856
	B [J/mol]	46.031	53.789	54.699
Sips $q_e = \frac{q_m (b_S c_e)^n}{1 + (b_S c_e)^n}$	r^2	0.999	0.997	0.999
	q_m [mg/g]	380.27	521.14	538.81
	b_S [dm^3/mg]	0.029	0.018	0.050
	n	0.713	0.619	0.602
Brouers–Sotolongo $q_e = q_m(1 - e^{(-K_w C_e^{\alpha})})$	r^2	0.999	0.997	0.999
	q_m [mg/g]	325.37	416.78	452.25
	Kw [(mg/g) (dm^3/mg)$^{1/\alpha}$]	0.105	0.108	0.191
	α	0.596	0.551	0.516

RH to transfer from the bulk solution onto and into the solid particle. With the increase of ultrasound power, sorption rate is increased due to reduced mass transfer resistances. The parameters K_{id1} and K_{id2} indicate that film diffusion is more efficient than intraparticle diffusion for all ultrasound powers. C_1 and C_2 were proportional to the boundary layer thickness and increased with initial concentration, larger C value corresponding to a greater boundary layer. The values of C decrease with increase of ultrasound power.

Values of parameters for Chrastil's model determined by nonlinear regression analysis are given in Table 1. The value of diffusion resistance coefficient (n) is <0.5, which indicates that the mechanism of sorption process is strongly limited by diffusion resistance.

Sorption isotherms

Five isotherm models were used to estimate which model fits best experimental data and provide an insight into the sorption mechanism, the surface properties, and affinity of the sorbent.

The fitted results and corresponding parameters of RH sorption on LSAC are shown in Fig. 7 and Table 2. From Table 2 it can be seen that the coefficients of determinations (r^2) obtained for the Langmuir isotherm model in the studied concentration ranges were high ($r^2 > 0.98$) at all ultrasound powers, but not the greatest. The maximum sorption capacity predicted by the Langmuir isotherms for all ultrasound powers was approximately the same as the experimentally obtained values of maximum sorption capacity of LSAC for RH. The simple Langmuir isotherm assumes monolayer sorption onto a uniform sorbent surface containing a finite number of sorption sites with a similar binding energy level.

The maximum sorption capacities of LSAC for RH calculated from the Langmuir model at the ultrasound powers of 0, 25, and 50 W were 328.71, 389.84, and 425.43 mg/g[1] (20°C), respectively. The experimentally determined values of maximum sorption capacities were 310.72, 369.12, and 423.87 mg/g[1] at the ultrasound powers of 0, 25, and 50 W, respectively. These results indicate that the sorption capacity increases for about 30% with an increasing of acoustic power from 0 to 50 W. The amount of sorbed RH by LSAC increased with the increases of RH concentration in the equilibrium solution. The values for the Langmuir sorption constant K_L increased with increasing ultrasound power. We can conclude that ultrasound positively affects the sorption affinity of LSAC for RH.

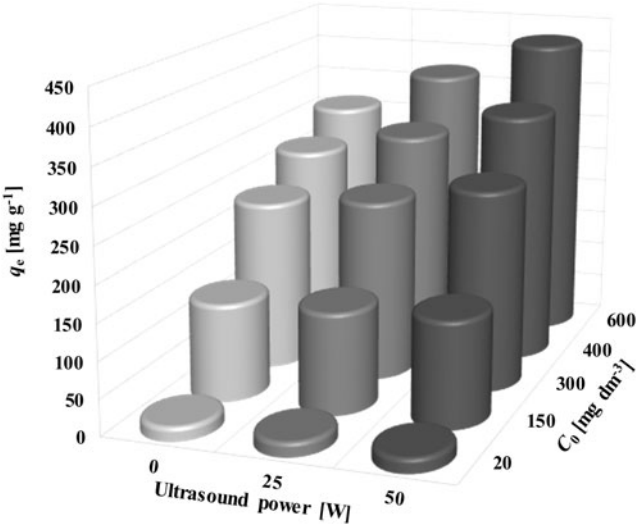

FIG. 8. Effect of initial concentration of amount of RH sorbed at equilibrium using different ultrasound power. Initial concentration from 20 to 600 mg/dm^3, sorbent dose 1.0 g/dm^3, acoustic power 0, 25, and 50 W, stirring speed 200 rpm, and temperature 20°C.

Table 3. Comparison of Maximum Sorption Capacity of LSAC for Ranitidine Hydrochloride and Other Parameters with Some Reported Data in the Literature

Sorbents	*pH*	*Sorbent dose [g/dm^3]*	*Sorption capacities [mg/g]*	*Maximum used RH concentration [mg/dm^3]*	*References*
LSAC (sorption with ultrasound)	2–11	1	446.75	600	Present study
Parthenium hysterophorus derived activated N-biochar	2	0.05	400	200	Mondal *et al.* (2017)
LSAC (sorption without ultrasound)	2–11	1	329.1	600	Present study
Natural cellulose	11	0.02	32.9	1000	Bezerra *et al.* (2014)
Activated carbon from mung bean husk	2	0.75	28	100	Mondal *et al.* (2015)
Graphene oxide	11	2	3.96	10	Das and Das (2016)

RH, ranitidine hydrochloride.

Table 4. Calculated Thermodynamic Parameters for Sorption of Ranitidine Hydrochloride onto LSAC

	Ultrasound power 0 W			*Ultrasound power 25 W*			*Ultrasound power 50 W*		
Parameter	*283* K	*293* K	*303* K	*283* K	*293* K	*303* K	*283* K	*293* K	*303* K
q_{max} [mg/g]	329.10	310.72	296.26	381.72	369.12	345.63	446.75	423.87	411.48
ln K_D	1.2148	1.0741	0.9754	1.7488	1.5988	1.3588	2.9153	2.4067	2.1827
$\Delta G°$ [J/mol]	–457.87	–168.29	58.66	–1381.4	–1104.0	–789.6	–2517.5	–2066.4	–1836.5
$\Delta H°$ [kJ/mol]	–7.84			–8.96			–10.36		
$\Delta S°$ [J/mol·K]	–26.10			–26.74			–27.81		
r^2 [ln K_D/1/T]	0.995			0.994			0.946		

The separation factor (R_L) values indicate the type of the isotherm and may be unfavorable ($R_L > 1$), linear ($R_L = 1$), favorable ($0 < R_L < 1$), or irreversible ($R_L = 0$) (Sivarajasekar *et al.*, 2017d). In this study R_L values were between 0 and 1, indicating that RH sorption on LSAC was favorable for all values of ultrasound power. The determination coefficients for Sips and Brouers-Sotolongo isotherm models are relatively similar or larger compared to those of Langmuir models. However, the experimentally obtained q_m values did not agree with the calculated q_m values obtained from the Freundlich and Sips isotherm models, for which a reasonable explanation could not be given in the present study.

From Table 2, it was observed that beside the Langmuir model, the Brouers-Sotolongo isotherm model gives the best fit to the experimental data, which indicates the presence of active sites with heterogeneous sorption interactions. Based on values α (being related to the heterogeneity $\alpha < 1$) it can be inferred that the sorption environment in LSAC material was heterogeneous.

However, q_m values obtained from the Brouers-Sotolongo model for all applied ultrasound powers were approximately similar to the experimentally obtained values. The equilibrium experimental data were fitted also by the Temkin isotherm model. The Temkin sorption potential K_T indicates high LSAC affinity for RH, probably due to its large ionic radius. The Temkin constant B indicates that interactions between LSAC and RH represent the physical sorption process (Fig. 8; Aytas *et al.*, 2011).

For the purpose of comparison, Table 3 presents the maximum sorption capacity of LSAC for RH and other parameters in our study, with some data for different sorbents reported in the literature.

The great advantage of this sorbent, in addition to higher sorption capacity, is the possibility of efficient removal of RH in a very wide pH range (from 2 to 11), unlike many of the previously used sorbents, which is given in our previous study of authors Bojić *et al.* (2015).

Thermodynamic study

Values for $\Delta G°$, $\Delta H°$, and $\Delta S°$ at different temperatures (283, 293, and 303 K) and acoustic powers (0, 25, and 50 W)

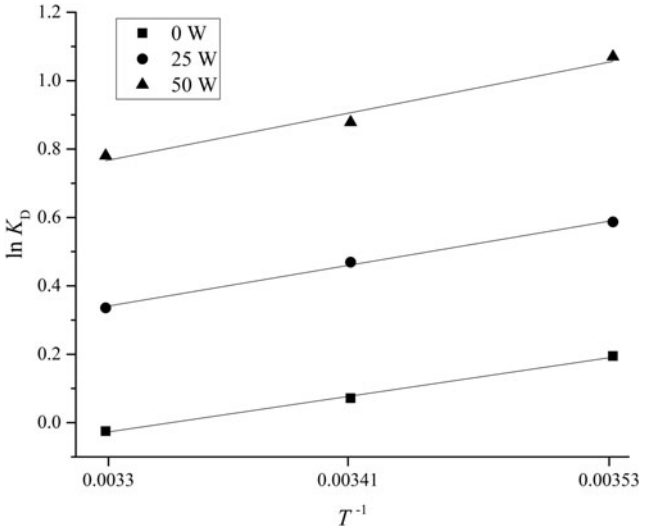

FIG. 9. Plot of ln K versus 1/T for estimation of thermodynamic parameters for the sorption of RH onto LSAC.

are given in Table 4. The values of $\Delta G°$ are negative and indicate a thermodynamically favorable spontaneous process with high affinity of LSAC for RH. $\Delta G°$ values are in the range from 58.66 to −2517.47 J/mol corresponding to physisorption, which is in accordance with previous presented isotherm study (Hao *et al.*, 2017). In addition, Gibbs energy of process is more negative with an increase of temperature and ultrasound power, indicating increase of sorption spontaneity with these parameters.

The small negative values of $\Delta H°$ indicate that the sorption process is slightly exothermic, or almost without enthalpy changes. Decrease of the sorption capacity with increasing of temperature (Table 4) might be due to physical nature of sorption mechanism, which is characterized by desorption on higher temperatures. The negative values of $\Delta S°$ at all temperatures and all acoustic powers suggest a decrease in the randomness at the solid/solution interface during the sorption process. In the presence of ultrasound, values of $\Delta S°$ slightly decreased, which may indicate that ultrasound cannot disrupt the sorbent particles and cannot change the morphology of the surface (Fig. 9).

Conclusion

The possibility of improvement of sorption removal of RH by activated carbon with the assistance of ultrasound was investigated in the present study. Detailed characterization of LSAC by BET, Boehm's, pH_{PZC}, FTIR, SEM, and EDS analysis was performed. Results show that the influence of ultrasound on the sorption of RH has a dual effect in comparison to silent sorption: it increases the rate of the sorption process and enhances the sorption capacity of LSAC. Several parameters such as acoustic power, stirring speed, sorbent dosage, temperature, contact time, and initial concentration were found to affect RE of RH.

The sorption capacity obtained from the nonlinear Langmuir model increases for about 30% with increase of acoustic power from 0 to 50 W. This phenomenon can be explained by significant increasing of efficiency of RH molecule diffusion in LSAC micropores. The sorption of RH on LSAC was best fitted by Langmuir model, which implies monolayer sorption. The nonlinear pseudo-second order and Chrastil's models were the most useful for describing the kinetics of RH sorption on LSAC for all powers of ultrasound and temperatures. The sorption processes were slightly exothermic, spontaneous, and feasible in nature. The mechanism of RH sorption on LSAC was physisorption. Based on the examined parameters it can be concluded that ultrasound significantly improves RH RE, whereas sorption efficiency is inversely proportional to temperature.

These data can be useful for designing a sorption scheme for the removal of RH and other drugs or similar organic molecules from aqueous solution.

Acknowledgment

This work was financed by the Serbian Ministry of Education, Science and Technological Development through the Grant No. TR34008.

References

Adewuyi, Y.G. (2001). Sonochemistry: Environmental science and engineering applications. *Ind. Eng. Chem. Res*. 40, 4681.

Aytas, S., Turkozu, D.A., and Gok, C. (2011). Biosorption of uranium(VI) by bi-functionalized low cost biocomposite adsorbent. *Desalination* 280, 354.

Baccar, R., Sarrà, M., Bouzid, J., Feki, M., and Blánquez, P. (2012). Removal of pharmaceutical compounds by activated carbon prepared from agricultural by-product. *Chem. Eng. J.* 211–212, 310.

Bergheim, M., Gieré, R., and Kummerer, K. (2012). Biodegradability and ecotoxicitiy of tramadol, ranitidine, and their photoderivaives in the aquatic environment. *Environ. Sci. Poll. Res*. 19, 72.

Bezerra, R.D.S., Silva, M.M.F., Morais, A.I.S., Santos, M.R.M.C., Airoldi, C., and Filho, E.C.S. (2014). Natural cellulose for ranitidine drug removal from aqueous solutions. *J. Environ. Chem. Eng.* 2, 605.

Bojić, D., Momčilović, M., Milenković, D., Mitrović, J., Banković, P., Velinov, N., and Nikolić, G. (2015). Characterization of a low cost Lagenaria vulgaris based carbon for ranitidine removal from aqueous solutions. *Arab. J. Chem.* DOI:org/10.1016/j.arabjc.2014.12.018

Brouers, F., Sotolongo, O., Marquez, F., and Pirard, J.P. (2005). Microporous and heterogeneous surface adsorption isotherms arising from Levy distributions. *Physica A*. 349, 271.

Bui, T.X., and Choi, H. (2010). Influence of ionic strength, anions, cations, and natural organic matter on the adsorption of pharmaceuticals to silica. *Chemosphere* 80, 681.

Chrastil, J. (1990). Adsorption of direct dyes on cotton: Kinetics of dyeing from finite baths based on new information. *Text. Res. J.* 60, 413.

Das, P., and Das, P. (2016). Graphene oxide for the treatment of ranitidine containing solution: Optimum sorption kinetics by linear and non linear methods and simulation using artificial neural network. *Process Saf. Environ. Protec.* 102, 589–595.

Dezotti, M., and Bila, D.M. (2003). Farmacos no meio ambiente. *Quim. Nova* 26, 523.

Entezari, M.H., and Bastami, T.R. (2006). Sono-sorption as a new method for the removal of lead ion from aqueous solution. *J. Hazard. Mater.* 137, 959.

Entezari, M.H., and Keshavarzi, A. (2001). Phase-transfer catalysis and ultrasonic waves. II. Saponification of vegetable oil. *Ultrason. Sonochem.* 8, 213.

Figueroa, R.A., Leonard, A., and MacKay, A.A. (2004). Modeling tetracycline antibiotic sorption to clays. *Environ. Sci. Technol.* 38, 476.

Guechi, E.K., and Hamdaoui, O. (2016). Sorption of malachite green from aqueous solution by potato peel: Kinetics and equilibrium modeling using non-linear analysis method. *Arab. J. Chem.* 9, 416.

Hamdaoui, O., Naffrechoux, E., Tifouti, L., and Pétrier, C. (2003). Effects of ultrasound on adsorption-desorption of p-chlorophenol on granular activated carbon. *Ultrason. Sonochem.* 10, 109.

Hao, R., Wang, P., Wu, Y., Hu, R., Zhang, J., and Song, Y. (2017). Impacts of water level fluctuations on the physicochemical properties of black carbon and its phenanthrene adsorption-desorption behaviors. *Ecol. Eng.* 100, 130.

Ho, Y.S., and McKay, G. (1998). Kinetic models for the sorption of dye from aqueous solution by wood. *Process Saf. Environ. Prot.* 76, 183.

Kaouah, F., Boumaza, S., Berrama, T., Trari, M., and Bendjama, Z. (2013). Preparation and characterization of activated carbon from wild olive cores (oleaster) by H_3PO_4 for the removal of Basic Red 46. *J. Clean. Prod.* 54, 296.

Kimura, T., Sakamoto, T., Leveque, J.M., Sohmiya, H., Fujita, M., Ikeda, S., and Ando T. (1996). Standardization of ultrasonic power for sonochemical reaction. *Ultrason. Sonochem*. 3, 157.

Krika, F., Azzouz, N., and Ncibi, M.C. (2016). Adsorptive removal of cadmium from aqueous solution by cork biomass: Equilibrium, dynamic and thermodynamic studies. *Arab. J. Chem.* 9, 1077.

Kyzas, G.Z., Kostoglou, M., Lazaridis, N.K., Lambropoulou, D.A., and Bikiaris, D.N. (2013). Environmental friendly technology for the removal of pharmaceutical contaminants from wastewaters using modified chitosan adsorbents. *Chem. Eng. J.* 222, 248.

Lagergren, S. (1898). About the theory of so-called adsorption of soluble substances [in German]. *K. Vet. Akad. Handl*. 24, 1.

Martucci, A., Pasti, L., Marchetti, N., Cavazzini, A., Dondi, F., and Alberti, A. (2012). Adsorption of pharmaceuticals from aqueous solutions on synthetic zeolites. *Microporous Mesoporous Mater*. 148, 174.

Mason, T.J., Paniwnyk, L., and Lorimer, J.P. (1996). The uses of ultrasound in food technology. *Ultrason. Sonochem*. 3, 253.

Mondal, S., Aikat, K., Siddharth, K., Sarkar, K., DasChaudhury, R., Mandal, G., and Halder, G. (2017). Optimizing ranitidine hydrochloride uptake of Parthenium hysterophorus derived N-biochar through response surface methodology and artificial neural network. *Process. Saf. Environ. Prot.* 107, 388.

Mondal, S., Sinha, K., Aikat, K., and Halder, G. (2015). Adsorption thermodynamics and kinetics of ranitidine hydrochloride onto superheated steam activated carbon derived from mung bean husk. *J. Environ. Chem. Eng.* 3, 187.

Omri, A., Wali, A., and Benzina, M. (2016). Adsorption of bentazon on activated carbon prepared from Lawsonia inermis wood: Equilibrium, kinetic and thermodynamic studies. *Arab. J. Chem.* 9, 1729.

Sips, R. (1948). On the structure of a catalyst surface. *J. Chem. Physics*. 16, 490.

Sivarajasekar, N., Baskar, R., Ragu, T., Sarika, K., Preethi, N., and Radhika, T. (2017c). Biosorption studies on waste cotton seed for cationic dyes sequestration: Equilibrium and thermodynamics. *Appl. Water Sci.* 7, 1987.

Sivarajasekar, N., Mohanraj, N., Balasubramani, K., Maran, J.P., Moorthy, I.G., Karthik, V., and Karthikeyan, K. (2017b). Optimization, equilibrium and kinetic studies on ibuprofen removal onto microwave assisted–activated Aegle marmelos correa fruit shell. *Desal. Wat. Treat.* 84, 48.

Sivarajasekar, N., Mohanraj, N., Baskar, R., and Sivamani, S. (2017a). Fixed-bed adsorption of ranitidine hydrochloride onto microwave assisted—Activated aegle marmelos correa fruit shell: Statistical Optimization and Breakthrough Modelling. *Arab. J. Sci. Eng*. DOI:org/10.1007/s13369-017-2565-4

Sivarajasekar, N., Paramasivan, T., Muthusaravanan, S., Muthukumaran, P., and Sivamani, S. (2017d). Defluoridation of water using adsorbents-A concise review. *J. Environ. Biotechnol. Res*. 6, 186.

Taleb, K., Markovski, J., Veličković, Z., Rusmirović, J., Rančić, M., Pavlović, V., and Marinković, A. (2016). Arsenic removal by magnetite-loaded amino modified nano/microcellulose adsorbents: Effect of functionalization and media size. *Arab. J. Chem.* DOI:org/10.1016/j.arabjc.2016.08.006

Tejeda, A., Torres-bojorges, Á.X., and Zurita, F. (2017). Carbamazepine removal in three pilot-scale hybrid wetlands planted with ornamental species. *Ecol. Eng.* 98, 410.

Temkin M.I., and Pyzhev, V. (1940). Kinetics of ammonia synthesis on promoted iron catalyst. *Acta Physica et Chimia USSR.* 12, 327.

Vediappan, K., and Lee, C.W. (2011). Electrochemical approaches for the determination of ranitidine drug reaction mechanism. *Curr. Appl. Phys.* 11, 995.

Zhou, S.K., Liu, Y.J., Jiang, H.Y., Deng, W.J., and Zeng, G.M. (2017). Adsorption of U(VI) from Aqueous Solution by a Novel Chelating Adsorbent Functionalized with Amine Groups: Equilibrium, Kinetic, and Thermodynamic Studies. *Environ. Eng. Sci.* DOI:org/10.1089/ees.2017.0017